

Fractionated stellar wind and the H/He abundance anomalies in Bp stars

K. Hunger¹ and D. Groote²

¹ Institut für Astronomie und Astrophysik, Universität Kiel, Leibnizstrasse, Physikzentrum, 24098 Kiel, Germany

² Hamburger Sternwarte, Gojenbergsweg 112, 21029 Hamburg, Germany

Received 20 April 1999 / Accepted 10 September 1999

Abstract. Radiatively driven winds occur in all main sequence stars (Babel 1995, 1996). However, due to the weak coupling between the photon absorbing metals and the *inert* elements H and He, the wind in the low temperature domain is fractionated: He decouples from the wind at $T_{\text{eff}} < 25\,000$ K, and below 17 000 K even H. The decoupled elements fall back to the surface of the star thus creating overabundances and abundance stratifications. These anomalies, however, become manifest only if atmospheric turbulence is suppressed (say by magnetic fields).

In order to prove the validity of the described scenario, all B_p stars for which reliable fundamental parameters exist, are discussed on the basis of the (augmented) (g, T_{eff})-diagram of Babel (1996). It is shown that the fractionation process is able to explain the observed temperature sequence of He-rich and He-poor stars, additionally to classical diffusion processes. A necessary condition is that a magnetic field is present. This explains why only a fraction of B stars exhibits H/He anomalies. While classical diffusion operates in the quiet zones (no wind) of a star, fractionation takes place above the wind bases.

Key words: stars: abundances – stars: chemically peculiar – stars: mass-loss

1. Introduction

Multicomponent hydrodynamical model atmospheres of the sun and stars have been considered in connection with abundance anomalies in atmospheres and winds. Johnson (1925) and Milne (1926) discussed the possibility that ions could escape from the atmospheres of stars.

Geiss et al. (1970) studied the problem whether the observed abundance anomalies in the solar wind and corona can be ascribed to differences in the coupling strengths of the various ions considered. (In this model, the flux of the proton is considered the agent that drives the other ions, including helium.) It is shown that the heavier elements do not attain proton velocities, and that substantial isotopic fractionation is possible, in particular regarding helium.

In hot stars, the wind is driven by radiation, the latter being absorbed by metal ions. Coulomb interaction between these ions and the passive elements hydrogen and helium then determines whether a homogeneous wind, i.e. a one component wind can develop. Castor et al. (1975) concluded that Coulomb interaction forces all species to move with the same velocity. Michaud et al. (1987), however, showed that in the presence of mass loss, the He abundances in the line-forming depths may be modified by chemical separation that takes place not only in the atmosphere but also in the wind and in the envelope of the star. In their models, both He-rich and H-rich winds are considered. In the latter case, a pure proton (coronal) wind is computed first, and then the friction between α -particles and protons is taken into account. Friction may lead to *differential winds* (*selective mass losses*) and thus to He-enrichment in the photosphere, whenever friction is small, i.e. when the mass loss rate is smaller than $3 \cdot 10^{-13} M_{\odot} \text{ yr}^{-1}$, at $T_{\text{eff}} = 25\,000$ K for instance.

Element fractionation in the solar chromosphere is known since 1963 (Pottasch). Elements with the first ionization potential below 10 eV (low FIP elements) are enriched in comparison to high FIP elements by as much as a factor of 4 for slow winds, whereas in fast winds a factor of 2 is reached. A simple ionization-diffusion model is proposed by Peter (1998) that explains the observed elemental fractionations, especially their dependence on the wind velocity. Drake et al. (1995, 1997) and Laming et al. (1996) studied the abundances in the coronae of Procyon, ϵ Eridani and α Centauri, on the basis of EUVE spectrograms to check whether the FIP-effect is also present in (cool) stars. This proved to be the case namely for α Cen, and to a lesser degree also to ϵ Eri, while no fractionation is detected in Procyon.

Springmann & Pauldrach (1992) demonstrated that in thin radiatively driven winds (small mass loss rates, large velocities), friction between the photon absorbing metal ions and the passive elements hydrogen and helium does not necessarily lead to single-velocity winds. Differential acceleration may cause appreciable drifts between ions and the *bulk matter*. The ions in that case, fully decouple - via *ion stripping* - from the rest and leave the star at high velocities (run away case, metallic wind).

Hunger et al. (1990, 1996), Hunger & Groote (1992), and Groote & Hunger (1997) studying the photospheric abundances

Send offprint requests to: K. Hunger

Correspondence to: dgroote@hs.uni-hamburg.de

of the (hot) magnetic rotator σ Ori E came to the conclusion that He-enrichment in patches of the stellar surface must also be related to fractionation of the wind. The wind again is anticipated to be driven by radiation.

Babel (1995, 1996), also on the basis of ion stripping considers the onset and existence of radiatively driven winds in main sequence A and B stars. He assumes a 3 component fluid consisting of protons, metal ions, and electrons. Full dependence of the radiative acceleration on the outward velocity of the metals is taken into account. By means of simple but efficient criteria involving the amount of radiative acceleration at the sonic point and at the critical point of hydrogen respectively, he is able to predict at which effective temperature and/or gravity (*i*) only negligible (metallic) winds are possible, (*ii*) inhomogeneous (fractionated) winds occur, and (*iii*) homogeneous (one component) winds develop. The remarkable result is that radiatively driven winds may be expected down to $T_{\text{eff}} = 10^4 \text{ K}$ (though with negligible small mass loss rates (case *i*). The metal winds occur at large gravities, for a given T_{eff} . They can hardly be observed directly, as the metals attain escape velocities ($> 1000 \text{ km s}^{-1}$) and consequently have low densities.

Case *ii*, however, leads to interesting and observable phenomena: at the critical point of hydrogen only about one half of the protons are still coupled to the driving metals¹. As the decoupled protons do not experience forces other than gravity (besides eventual magnetic forces), they are forced back to the surface of the star, thus creating overabundances of hydrogen (H-rich stars) and also abundance stratifications (Farthmann et al. 1994). The wind that eventually leaves the star, hence, is predominantly metallic, as in case *i*.

In case *iii*, the total radiative acceleration exceeds gravity even at the sonic point. The wind is homogeneous, and no wind induced abundance anomalies can be expected (classical wind domain).

The above described domains in the (g, T_{eff}) -diagram remarkably well describe the observed distribution of hydrogen anomalous stars (see below). Therefore it appears worthwhile to probe whether fractionation of helium may equally well describe the observed distribution of helium rich stars. In Sect. 2, the original Babel diagram is augmented in order to include helium. In Sect. 3, this diagram is discussed on hand of new data concerning effective temperatures (Groote 1982) and gravities of CP stars. The data are derived exclusively by means of the infrared flux method (T_{eff} , Blackwell & Shallis 1977) and HIPPARCOS parallaxes ($\log g$) and thus form a homogeneous sample largely free of systematic errors. They comprise He-rich as well as He-poor stars. Sect. 4 is addressed to the important issue as to the validity and interrelation of the two mechanism that modify photospheric abundances, namely classical diffusion and wind induced fractionation.

¹ This, however, does not necessarily mean that all of these protons will eventually reach escape velocity and thus leave the star, as the Babel conditions are necessary but not sufficient. Especially, they do not take into account density gradients which are important since metals and protons are coupled via Coulomb collisions, the latter being proportional to the square of the density.

2. Fractionated stellar winds and the HR diagram

2.1. Hydrogen

Fractionated (multicomponent) winds may be found in main sequence A and B stars within a range of $\Delta \log g = 0.36$, for given T_{eff} (Babel 1996). The lower bound g_l is defined by the condition that at the sonic point, the total radiative acceleration $g_{\text{rad}}^{\text{tot}}$ (i.e. averaged over the whole wind ensemble consisting of hydrogen and metals) equals stellar gravity g , while the upper bound g_u is defined by the condition that $g_{\text{rad}}^{\text{tot}}$ is smaller than g at the sonic point, but larger than g at the critical point of hydrogen, r_c^{H} . At the critical point, the velocity of the (photon absorbing) metal ions u_m does not exceed the velocity of the (inert) H ions by more than $\sqrt{2} \cdot a_{\text{H}}$, with $a_{\text{H}} = \sqrt{kT/m_{\text{H}}}$, otherwise the momentum transfer from metals to hydrogen becomes inefficient. At r_c^{H} , only 57% of the protons remain coupled to the metals. Stars with $g < g_l$ are supposed to develop homogeneous winds, while stars with $g > g_u$ have only metallic winds.

Momentum exchange between metals and hydrogen takes place via Coulomb interaction the latter being proportional to the number fraction G_1 of (thermally distributed) metal ions and protons that have common velocities, when there is a velocity drift $\Delta u = X \cdot \sqrt{2} \cdot a_{\text{H}}$ between the bulks of the two components. $G_1(X)$ is related to Chandrasekhar's function $G(X)$ that describes the energy exchange between the two components (Chandrasekhar 1941): $G(X) = 0.376 X \cdot G_1(X)$. $G_1(X)$ is unity at $X = 0$, and declines rather slowly with X , as $G_1(X) \approx 0.568 X^{-1.1}$ at $X = 1$, for instance. Instead of using a single cut off, namely $X = 1$, i.e. $G_1 = 0.568$ as Babel proposes, we introduce a second cut off $X = 1.6$, i.e. $G_1(X) = 0.272$ that may be used alternatively. (This means that we introduce a second critical point of hydrogen, however, as the wind temperature is assumed to be independent of height, r_c^{H} is undetermined.) For simplicity, we redefine the lower bound g_l by the condition $X = 0 (G = 1.0)$ which yields almost the same accelerations as Babel's condition does (see below).

As we have seen above, the upper and lower bounds depend on the radiative acceleration of the metals, $g_{\text{rad},m}$, as well as on the mass fraction of the particles carried by the wind. $g_{\text{rad},m}$ can be read off Babel's (1996) velocity/gravity diagram which is based on the assumptions: $T_{\text{wind}} = T_{\text{eff}}$ and electron density $n_e/W = 2 \cdot 10^{10} \text{ cm}^{-3}$. According to this diagram, $g_{\text{rad},m}$ varies with u_m like $\Delta \log g_{\text{rad},m} \approx 1.2 \Delta \log u_m$ ($T_{\text{eff}} \approx 20\,000 \text{ K}$), almost independently of density. For $g_{\text{rad}}^{\text{tot}}$ we have the simple relation: $\Delta \log g_{\text{rad}}^{\text{tot}} = -\Delta \log(\text{mass fraction})$. We shall use these relations below.

The (hydrogen) curves are shown in Fig. 1 (dashed). The curve labelled $G = 1.0$ marks the lower bound of g which agrees within $\Delta \log g \approx 0.05$ with Babel's dividing line. $G = 0.57$ corresponds to Babel's upper bound, however, differs by as much as $\Delta \log g = +0.23$ (for $T_{\text{eff}} > 17000 \text{ K}$). The reason for the discrepancy lies in the definition of the dividing lines: Babel's curve describes the *on set* phase of the wind, with full participa-

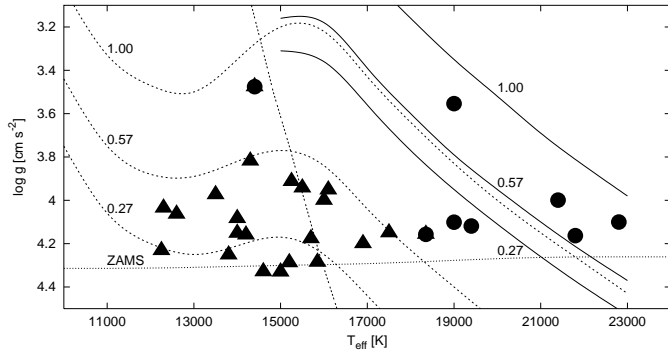


Fig. 1. $\log g/T_{\text{eff}}$ -diagram for He-rich and H-rich (He-poor) stars. *Dashed lines* are derived from Babel’s diagram with 100%, 57%, and 27% (from top to bottom) of hydrogen coupled to metals, no helium included. *Full drawn lines* are calculated for a mixed atmosphere with initially solar composition. Filled circles belong to He-rich and triangles to H-rich stars respectively. The transition where helium is partially ionized $n_{\text{He}^+}/(n_{\text{He}^+} + n_{\text{He}}) = 0.7$ (see Heber 1998) is marked by a straight line (dashed), near 15 000 K. For details see text.

tion of hydrogen, while our curve refers to the *stationary* case, in which hydrogen is reduced to 57%² – see also Sect. 3.1.

2.2. Helium

Adding helium means that we have to consider a three component wind, consisting of H, He, and metals. However, if we neglect the coupling between protons and helium ions – which is justified in view of the number of approximations implicitly introduced elsewhere (neglect of density etc.), see also Springmann & Pauldrach (1992), and Springmann (1994) – we proceed as in Sect. 2.1: At the critical points of helium r_c^{He} , the velocity of the metal ions u_m does not exceed the velocity of the helium ions by more than $\Delta u = X \cdot \sqrt{2} \cdot a_{\text{He}}$, with $a_{\text{He}} = \sqrt{kT/m_{\text{He}}}$. $X = 0$ defines the lower bound g_l , below which He is supposed to be fully coupled, while at $X = 1$ and $X = 1.6$, only the fraction $G_1 = 0.568$ and 0.272 respectively is coupled to the metals. As all velocities are smaller by a factor of 2 with respect to hydrogen, the resulting accelerations $g_{\text{rad},m}$ of the metals, again read off Babel’s (1996) diagram, are smaller by $\Delta \log g_{\text{rad},m} \approx 1.2 \Delta \log u_m = 0.36$.

So far, the presence of hydrogen is ignored. The mass fraction of hydrogen comes in when the total radiative acceleration of the wind ensemble is calculated. As hydrogen is (practically) fully coupled to the metals in those domains of the (g, T_{eff}) -diagram where the (fractionated) wind of helium becomes important, a *solar* mass fraction of hydrogen can be assumed. This leads to a further reduction of $\Delta \log g = 0.15$. For $G_1 = 1$ (upper bound for a full, one component wind) it means a total shift of $\Delta \log g = -0.5$ (see Fig. 1).

Other than in the case of hydrogen which is fully ionized in the whole temperature domain discussed, the ionization of helium has to be considered. Neutral helium ($Z = 0$) is not cou-

² Furthermore, Babel uses a ten times higher density which though, has small effects on the dividing lines.

pled to the metals, while doubly ionized helium ($Z = 2$) is even stronger coupled than the protons. The temperature range in which He-fractionation can occur, hence, is limited to approximately $15\,000\text{ K} < T_{\text{eff}} < 25\,000\text{ K}$. For illustration, the locus of stars which have an ionization fraction $n_{\text{He}^+}/(n_{\text{He}^+} + n_{\text{He}}) = 0.7$ (for $\tau_{4000} = 0.6$ from LTE model atmospheres (Heber 1998)) is reproduced (Fig. 1, straight line at $\approx 15\,500\text{ K}$). He-rich stars should not show up too far to the left of this line. A similar upper boundary defined by the second ionization of He lies near $30\,000\text{ K}$ (outside the diagram).

2.3. Reaccretion and question of stationarity

As was stated before: the fraction of inert particles (H or He) that are not coupled at the critical point and those which are decoupled further out because they do not attain escape velocities, are forced by gravity back to the surface of the star (reaccretion) thus leading to overabundances and abundance gradients. If magnetic fields are present, reaccretion proceeds along the same trajectories as those of the ascending particles. In this case, the abundance anomalies should show up at the wind bases. In case of *hydrogen*, it means that the (photospheric) number fraction increases only slightly (from 90% up to 100%). Nevertheless, reaccreted H blankets the photosphere thus filling up He- and metal lines. Stars in the (g, T_{eff}) -domain with fractionated winds should be *He- and metal poor, with a solar He to metal ratio*.

The situation is different in case of *helium*: the He abundance observed in helium variables increases drastically, from 8% up to 100% locally, i.e. in the wind bases, and averaged over the visible surface to the order of 50% depending on the size of the wind bases. In this case, one obtains a *He-rich star that is H- and metal poor, with solar H to metal ratio*³.

But here, we encounter two problems: helium on top of an otherwise hydrogen dominated photosphere means a negative μ gradient which is known to be unstable against turbulent motions that might transport matter of original composition to the surface. A stabilizing force hence is needed that suppresses turbulence: the magnetic field. Hence we conclude that *all He-rich main sequence stars are also magnetic stars*, if the concept of fractionation is correct. This condition simultaneously answers the question, why only a small percentage of main sequence stars in the critical (g, T_{eff}) -domain are He-rich. More than one third of the He-rich stars indeed are known to have magnetic fields. (The others may have fields which are below the threshold of detection, but are large enough to prevent turbulence.) – A similar, perhaps less stringent condition might hold for H-rich stars.

The second problem concerns He-rich as well as He-poor stars: In both cases, the metals are depleted in the outer layers of

³ An interesting example may be the He-rich star HD 144941 (Harrison & Jeffery 1997). This star is not an extreme (evolved) He-star but exhibits a He-rich photosphere with hydrogen and metals depleted by 1.7 dex while the H/metal ratio is solar. HD 144941 is not variable. However, it cannot be excluded that the star is seen pole on, with a decentered dipole that is aligned with the axis of rotation.

Table 1. Data of stars shown in Fig. 1. *Top:* He-rich stars with He-rich patches and possibly H-rich and metal poor caps. *Bottom:* He-poor stars with only H-rich and metal poor (polar) caps. Stars are arranged in order of descending effective temperature. The two stars between the horizontal lines are intermediate cases, see text.

	T_{eff} [10^3 K]	$\log g$	M_* [M_{\odot}]	t 10^{-6} [yrs]
HD 64740	22.8 ± 0.6	$4.10^{+0.09}_{-0.08}$	$8.7^{+0.3}_{-0.3}$	11
HD 37776	21.8 ± 0.8	$4.16^{+0.30}_{-0.21}$	$7.8^{+1.1}_{-1.1}$	9
HD 96446	21.4 ± 1.2	$4.00^{+0.30}_{-0.23}$	$8.1^{+0.9}_{-0.9}$	19
HD 37017	19.4 ± 0.7	$4.12^{+0.34}_{-0.27}$	$6.5^{+0.7}_{-0.9}$	20
HD 58260	19.0 ± 0.4	$3.55^{+0.47}_{-0.27}$	$8.5^{+1.7}_{-2.0}$	28
HD 133518	19.0 ± 0.8	$4.10^{+0.20}_{-0.16}$	$6.4^{+0.4}_{-0.5}$	24
HD 125823	18.4 ± 0.4	$4.16^{+0.08}_{-0.11}$	$5.9^{+0.2}_{-0.2}$	21
HD 5737	14.4 ± 0.1	$3.48^{+0.15}_{-0.11}$	$5.5^{+0.4}_{-0.2}$	81
HD 142990	16.9 ± 0.5	$4.20^{+0.10}_{-0.09}$	$5.1^{+0.2}_{-0.2}$	21
HD 162374	16.1 ± 0.3	$3.95^{+0.18}_{-0.14}$	$5.2^{+0.4}_{-0.4}$	58
HD 142301	15.9 ± 0.3	$4.29^{+0.13}_{-0.11}$	$4.4^{+0.2}_{-0.3}$	5
HD 49333	15.7 ± 0.4	$4.18^{+0.12}_{-0.10}$	$4.6^{+0.2}_{-0.2}$	36
HD 109026	15.5 ± 0.3	$3.94^{+0.04}_{-0.04}$	$4.9^{+0.1}_{-0.1}$	66
HD 143699	15.2 ± 0.3	$3.91^{+0.10}_{-0.08}$	$4.9^{+0.2}_{-0.2}$	71
HD 144334	15.2 ± 0.5	$4.29^{+0.10}_{-0.09}$	$4.2^{+0.2}_{-0.2}$	6
HD 28843	15.0 ± 0.5	$4.33^{+0.08}_{-0.08}$	$4.0^{+0.1}_{-0.1}$	0
HD 90264	14.6 ± 0.5	$4.04^{+0.33}_{-0.10}$	$4.3^{+0.2}_{-0.6}$	76
HD 22920	14.3 ± 0.3	$3.82^{+0.13}_{-0.11}$	$4.7^{+0.3}_{-0.3}$	92
HD 74196	14.2 ± 0.6	$4.14^{+0.30}_{-0.05}$	$4.0^{+0.1}_{-0.5}$	63
HD 224926	14.0 ± 0.3	$4.08^{+0.07}_{-0.06}$	$4.0^{+0.1}_{-0.1}$	79
HD 146001	14.0 ± 1.0	$4.15^{+0.10}_{-0.09}$	$3.9^{+0.1}_{-0.1}$	65
HD 62712	13.8 ± 0.3	$4.25^{+0.08}_{-0.07}$	$3.7^{+0.1}_{-0.1}$	30
HD 22470	13.5 ± 0.4	$3.97^{+0.08}_{-0.09}$	$4.0^{+0.2}_{-0.2}$	107
HD 137509	12.6 ± 0.2	$4.06^{+0.12}_{-0.10}$	$3.5^{+0.2}_{-0.2}$	132
HD 27376	12.3 ± 0.4	$4.04^{+0.25}_{-0.02}$	$3.4^{+0.0}_{-0.3}$	150
HD 124224	12.2 ± 0.3	$4.23^{+0.06}_{-0.05}$	$3.1^{+0.1}_{-0.1}$	63

the star (Porter & Skouza 1999). This means that after the onset of the wind, and if the photospheric abundances of the metals decline *at the depths where the wind is initiated* as a result of the above mentioned (partial) accretion, the radiative acceleration also declines (in proportion to the metal abundances). In case, a star initially is close to the high gravity limit for the onset of the (fractionated) wind, the wind may be “extinguished”. In the intermediate gravity range, however, the wind continues at somewhat reduced rates and at reduced reaccretion rates until stationarity is reached. The curves in Fig. 1 are based on initial (solar) metal abundances. Metal depletion may shift the dividing lines to lower gravities.

3. ($\log g$, T_{eff})-distribution of H- and He-anomalous stars

In Table 1, gravities and effective temperatures of 18 He-poor and 8 He-rich stars are listed. Effective temperatures are taken from Groote (1982) and were derived by the infrared flux method (Blackwell & Shallis 1977) integrating fluxes from IR to UV. Gravities are determined from HIPPARCOS parallaxes together with tracks from stellar evolution (Schaller et al. 1992). Masses and ages are derived as a by-product and are reproduced

for the sake of completeness. The fundamental parameters are expected to be free of systematic errors.

3.1. Hydrogen

All program stars are located within coupling fractions 0.5 and 0.2, with a mean of 0.3. The mean accretion rate hence is 0.7. These numbers, however, refer to the onset phase, i.e. the phase when the abundances of the metals are still solar. Depending on the accretion rate and resulting reduced metal abundances, the loci of constant coupling fractions may shift towards lower gravities which in turn leads to smaller coupling fractions. However, neither the metal abundances in the wind bases are well known nor is the high gravity boundary for the onset of fractionated winds well defined (see Sect. 2). From Fig. 1, we conclude that a fractionated wind may be initiated even when the coupling fraction is only 0.2. From this follows that *all main sequence stars* with $14\,000 < T_{\text{eff}} < 25\,000$ K have *fractionated winds* which, however, may become manifest only when atmospheric turbulence is suppressed.

3.2. Helium

The 8 program stars (including intermediate cases) from Table 1 are spread over a wide range of coupling fractions, from 0.1 to 0.9, with a mean of 0.5. These numbers again refer to the onset phase of the wind. The small number of program stars may explain the rather large spread of coupling fractions. The mean gravity is $\log g = 4.0$, slightly lower than the gravity of H-rich stars ($\log g = 4.1$).

There are two stars which might be called intermediate cases (over plotted symbols in Fig. 1), because they are placed between the two groups above the 57% line for H-rich stars and below the 27% line for He-rich stars. HD 125823 varies between He-rich and He-poor and exhibits stratification (see Leone & Lanzafame 1997). HD 5737 is classified as He-poor and as sn-star (pointing also to stratification). It is H-rich at the magnetic pole and exhibits similar He equivalent width variations as σ Ori E (Groote et al. 1999) indicating He-rich spots, which cannot be excluded as the fraction of ionized helium is still above 30%. It seems to be a cool ($T_{\text{eff}}=14\,500$ K) analogue of σ Ori E ($T_{\text{eff}}=22\,500$ K) and is also known to be a ^3He star. According to T_{eff} the star should belong to the He-poor stars. However, the mass lies exactly between the two groups of stars.

4. Conclusions

Fractionation of the (radiatively driven) stellar wind is expected to occur in all main sequence B-stars, because the coupling via collisions between the metal ions and the *passive plasma* H and He becomes weak. H and/or He (depending on stellar gravity and effective temperature) decouple somewhere above the sonic point and are subsequently reaccreted by the star. This may lead to photospheric abundance anomalies and stratifications such as are observed in hot CP stars. A necessary condition, however, is that the photosphere is stable. (The condition is less stringent

for He-poor stars than for He-rich stars.) Hence one is led to conclude that *all He-rich stars and probably also all H-rich stars have magnetic fields*. This condition also would explain why only a (small) fraction of stars in the critical (g, T_{eff})-domain are CP stars. According to Table 1, the age of the CP stars ranges from 0 to 150 million years covering the entire main sequence time. This expresses that the CP phenomenon is not a transient feature.

In the magnetic case, the reaccreted material descends along the same trajectory as the ascending (wind) particles, thus leading to abundance anomalies at the wind bases (which is confirmed by observations – see Hunger & Groote (1992) and Groote & Hunger (1997)). The latter are located at or near the magnetic poles depending on the period of rotation and the inclination of the magnetic field. The wind velocities are too high to permit classical diffusion in the polar regions.

Classical diffusion, however, is dominant in the magnetic equatorial belt (Groote & Hunger 1997). This means that in one single magnetic stellar object both mechanisms that cause element segregation may be operative simultaneously, fractionation and classical diffusion.

Acknowledgements. We gratefully acknowledge the discussions with Drs. J. Babel, U. Springmann, A. Pauldrach, and J. Puls concerning fractionated winds.

References

- Babel J. 1995, A&A 301, 823
 Babel J. 1996, A&A 309, 867
 Blackwell D.E., Shallis M.J. 1977, MNRAS 180, 177
 Castor J., Abbott D., Klein R. 1975, ApJ 195, 157
 Chandrasekhar S. 1941, ApJ 93, 285
 Drake J.J., Laming J.M., Winding K.G. 1995, ApJ 343, 393
 Drake J.J., Laming J.M., Winding K.G. 1997, ApJ 478, 403
 Farthmann M., Dreizler S., Heber U., Hunger K. 1994, A&A, 291, 919
 Geiss J., Hirt P., Leutwyler H. 1970, Solar Physics, 12, 458
 Groote D. 1982, Ph.D., Technische Universität Berlin
 Groote D., Hunger K. 1982, A&A, 116, 64
 Groote D., Hunger K. 1997, A&A, 319, 250
 Groote D., Hunger K., Heber, U. 1999, (to be published later)
 Hamann W.R., 1981 (private communication)
 Harrison P.M., Jeffery C.S. 1997, A&A 323, 177
 Heber U., 1998 (private communication)
 Hunger K., Groote D. 1992, in Peculiar Versus Normal Phenomena in A-Type and Related Stars, IAU Coll. 138, eds. M.M. Dworetzky, F. Castelli, R. Farragiana, p.394
 Hunger K., Groote D., Heber U. 1996 in Hydrogen Deficient Stars, ASP Conference Series, Vol. 96, eds. C.S. Jeffery and U. Heber, p. 179
 Hunger K., Heber U., Groote D. 1990 in Properties of Hot luminous Stars, ASP Conference Series, Vol. 7, ed. C.D. Garmany, p. 307
 Johnson M.C. 1925, MNRAS 85, 813
 Laming J.M., Drake J.J., Winding K.G. 1996, ApJ 462, 948
 Leone F., Lanzafame A.C. 1997, A&A 320, 893
 Michaud G., Dupres J., Fontaine G., Montmérelle T. 1987, ApJ 322, 302
 Milne E.A. 1926, MNARS 85, 813
 Peter H. 1998, A&A 335, 691
 Porter J.M., Skouza B.A. 1999, A&A 344, 205
 Pottasch S.R. 1963, MNARS 125,543
 Schaller G., Schaerer D., Meynet G., Maeder A. 1992, A&AS 96, 269
 Springmann U.W.E., Pauldrach A.W.A. 1992, A&A 262, 515
 Springmann U.W.E. 1994, (private communication)

Note added in proof: After completion of our manuscript, an important paper came to our attention: *On the decoupling and reaccretion of low density, line driven winds*, Porter & Skouza (1999). The authors performed numerical 1D hydrodynamic simulations of the wind in a B2 V star. They were able to predict decoupling radii (of the order of $1.2 r_*$), decoupling velocities ($500\text{--}600 \text{ km s}^{-1}$) and stalling radii, i.e. where the velocity of the decoupled plasma reverses sign ($\approx 2\text{--}3r_*$). The decoupled plasma remains at the latter radius for a short time (hours/day) thus forming a shell before it finally contracts back to the surface. The shell is too thin to leave observable signatures. However, the authors argue that the process of reaccretion eventually will reduce metallicity in the outer layers of the star. Though the simulation is only at the 1D level and rotation and magnetic fields are not included, the results are remarkable in that metal depletion at the base of the wind is indeed observed (Groote & Hunger 1997) as well as the decoupling velocity $v_D = 600 \text{ km s}^{-1}$ (Hamann 1981). Both observations concern σ Ori E. There is also some observational evidence for reaccretion in this star. Scattered light from the decoupled hydrogen atoms can explain the additional absorptions observed above both polar caps (see Groote & Hunger 1997, Fig. 9).